

Directing Aryl–I versus Aryl–Br Bond Activation by Nickel via a Ring Walking Process

Olena V. Zenkina,[†] Amir Karton,[†] Dalia Freeman,[†] Linda J. W. Shimon,[‡] Jan M. L. Martin,^{*,†} and Milko E. van der Boom^{*,†}

Departments of Organic Chemistry and Chemical Research Support, The Weizmann Institute of Science, 76100 Rehovot, Israel

Received November 21, 2007

Activation of a strong aryl–Br bond of a halogenated vinylarene by nickel(0) is demonstrated in the presence of aryl–I containing substrates. η^2 -Coordination of Ni(PEt₃)₂ to the C=C moiety of halogenated vinylarenes is kinetically preferable and is followed by an intramolecular aryl–halide bond activation process. This “ring-walking” process is quantitative and proceeds under mild reaction conditions in solution. Mechanistic studies indicate that the metal insertion into the aryl–halide bond is not the rate-determining step. The reaction obeys first-order kinetics in the η^2 -coordination complexes with almost identical activation parameters for Br and I derivatives. The ring-walking process is kinetically accessible as shown by density functional theory (DFT) calculations at the PBE0/SDB-cc-pVDZ//PBE0/SDD level of theory.

Introduction

Metal-mediated aryl–halide bond activation is a key step in many carbon–carbon bond formation processes; examples include Stille, Suzuki, Heck, and Sonogashira reactions.^{1–5} Numerous experimental and theoretical studies have addressed the intriguing mechanism underlying aryl–halide oxidation addition by group 10 metals in solution.^{6–18} Regardless of the tremendous progress made in this field, many challenging open questions remain. To

date, selective activation of relatively strong chemical bonds in the presence of weaker ones is extremely rare.^{5,19–25} In particular, possible routes to selectively activate distinctly different aryl–halide bonds may be available by unimolecular reaction channels, which direct the metal center to the desired functional group as shown by van Koten et al.^{24,25} We recently demonstrated that the reaction of Pt(PEt₃)₄ with a halogenated vinylarene or azobenzene system results in selective η^2 -C=C or η^2 -N=N coordination, respectively, followed by “ring-walking” of the metal

* To whom correspondence should be addressed. E-mail: gershom@weizmann.ac.il (J.M.L.M.), milko.vanderboom@weizmann.ac.il (M.E.B.). Fax: +972-8-934-4142.

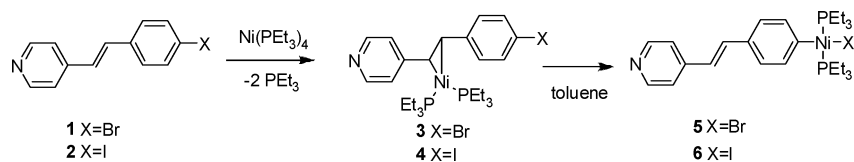
[†] Department of Organic Chemistry.

[‡] Department of Chemical Research Support.

- (1) Collman, J. P.; Hegedus, L. S.; Norton, J. R.; Finke, R. G. *Principles and Applications of Organotransition Metal Chemistry*; University Science Books: Mill Valley, CA, 2006.
- (2) Negishi, E. I. *Handbook of Organopalladium Chemistry for Organic Synthesis*; Wiley: New York, 2002.
- (3) Hegedus, L. S. *Transition Metals in the Synthesis of Complex Organic Molecules*; University Science Books: Mill Valley, CA, 1994.
- (4) Netherton, M. R.; Fu, G. C. *Adv. Synth. Catal.* **2004**, *346*, 1525.
- (5) van der Boom, M. E.; Milstein, D. *Chem. Rev.* **2003**, *103*, 1759.
- (6) Norrby, P.-O.; Ahlquist, M. *Organometallics* **2007**, *26*, 550.
- (7) Lam, K. C.; Marder, T. B.; Lin, Z. *Organometallics* **2007**, *26*, 758.
- (8) Lucassen, A. C. B.; Shimon, L. J. W.; van der Boom, M. E. *Organometallics* **2006**, *25*, 3308.
- (9) Gatard, S.; Celenligil-Cetin, R.; Guo, C. Y.; Foxman, B. M.; Ozerov, O. V. *J. Am. Chem. Soc.* **2006**, *128*, 2808.
- (10) Grushin, V. V.; Marshall, W. J. *J. Am. Chem. Soc.* **2006**, *128*, 4632.
- (11) Sharp, P. R.; Begum, R. A. *Organometallics* **2005**, *24*, 2670.
- (12) Dong, C.-G.; Hu, Q.-S. *J. Am. Chem. Soc.* **2005**, *127*, 10006.
- (13) Christmann, U.; Vilar, R. *Angew. Chem., Int. Ed.* **2005**, *44*, 366.

- (14) Sundermann, A.; Uzan, O.; Martin, J. M. L. *Chem.—Eur. J.* **2001**, *7*, 1703.
- (15) Hartwig, J. F. *Angew. Chem., Int. Ed.* **1998**, *37*, 2046.
- (16) Ohff, M.; Ohff, A.; van der Boom, M. E.; Milstein, D. *J. Am. Chem. Soc.* **1997**, *119*, 11687.
- (17) Zenkina, O.; Altman, M.; Leitun, G.; Shimon, L. J. W.; Cohen, R.; van der Boom, M. E. *Organometallics* **2007**, *26*, 4528.
- (18) Strawser, D.; Karton, A.; Zenkina, O. V.; Iron, M. A.; Shimon, L. J. W.; Martin, J. M. L.; van der Boom, M. E. *J. Am. Chem. Soc.* **2005**, *127*, 9322.
- (19) Espino, G.; Kurbangalieva, A.; Brown, J. M. *Chem. Commun.* **2007**, 1742.
- (20) Blum, J.; Berlin, O.; Milstein, D.; Ben-David, Y.; Wasserman, B. C.; Schutte, S.; Schumann, H. *Synthesis* **2000**, *4*, 571.
- (21) Littke, A. F.; Dai, C.; Fu, G. C. *J. Am. Chem. Soc.* **2000**, *122*, 4020.
- (22) van der Boom, M. E.; Liou, S.-Y.; Ben-David, Y.; Gozin, M.; Milstein, D. *J. Am. Chem. Soc.* **1998**, *120*, 13415.
- (23) Fahey, D. R. *J. Am. Chem. Soc.* **1970**, *92*, 402.
- (24) Slagt, M. Q.; Rodriguez, G.; Grutters, M. M. P.; Gebbink, R. J. M. K.; Klopper, W.; Jenneskens, L. W.; Lutz, M.; Spek, A. L.; van Koten, G. *Chem.—Eur. J.* **2004**, *10*, 1331.
- (25) Rodriguez, G.; Albrecht, M.; Schoenmaker, J.; Ford, A.; Lutz, M.; Spek, A. L.; van Koten, G. *J. Am. Chem. Soc.* **2002**, *124*, 5127.

Scheme 1. Selective η^2 -(C=C) Coordination of Ni(PEt₃)₂ to Compounds **1** and **2** is Followed by Activation of the Aryl–Halide Bond



center and rate-determining aryl–halide oxidative addition.^{17,18} Intramolecular pathways to arene functionalization have synthetic utility and can be utilized to selectively activate aryl–halide bonds.^{24–30} For example, Yokozawa et al. recently observed that nickel-catalyzed chain growth polymerization of poly(3-hexylthiophene) and poly(*p*-phenylene) proceeds by intramolecular transfer of the Ni(0) catalyst over the conjugated system, followed by selective activation of only one of the C–Br bonds.^{26–28}

We report here on the exclusive activation of a strong aryl–Br bond of a halogenated vinylarene by nickel(0) in the presence of aryl–I containing substrates. The experimental findings and mechanistic interpretation are supported by density functional theory (DFT) calculations at the PBE0/SDB-cc-pVDZ//PBE0/SDD level of theory.

Results and Discussion

The reaction of an equimolar amount of Ni(PEt₃)₄ with compounds **1** or **2** in dry toluene-*d*₈ at 271 K for ~80 min results in the quantitative formation of complexes **3** or **4**, respectively (Scheme 1). Compounds **3** and **4** were characterized in situ in the presence of 2 equiv of PEt₃ by low temperature ¹H, ¹³C{¹H}, and ³¹P{¹H} NMR spectroscopy. Assignments in the ¹³C{¹H} NMR spectra were made using ¹³C-DEPT-135 NMR spectroscopy. Although compounds **3** and **4** could not be isolated, their spectroscopic characteristics are nearly identical to those of isolated platinum complexes.^{17,18} Prolonged reaction times (~14 h) or increasing the reaction temperature results in the quantitative formation of complexes **5** and **6** by metal insertion into the aryl–halide bond. For instance, this reaction goes to completion in ~1.5 h at room temperature. The new Ni(II) complexes (**5**, **6**) have been isolated by evaporation of all the volatiles under vacuum and by washing with cold pentane as yellow solids (80%), and they were fully characterized by a combination of ¹H, ¹³C{¹H}, and ³¹P{¹H} NMR spectroscopy, elemental analysis, and mass spectrometry.³¹ In addition, complex **5** has been characterized by single-crystal X-ray crystallography (Figure 1). Evidently, selective η^2 -(C=C) coordination of Ni(PEt₃)₂ to compounds **1** and **2** is kinetically preferable over activation of the aryl–halide bond.

Mechanistically, the transformations of complexes **3** → **5** and **4** → **6** may proceed via reversible Ni(PEt₃)₂ dissociation

followed by intermolecular activation of the aryl–halide bond. No free ligands (**1**, **2**) or Ni(PEt₃)_{*x*} (*x* = 2–4) were observed during the course of the reactions by ¹H and ³¹P{¹H} NMR spectroscopy, indicating that the equilibrium is shifted toward complexes **3** and **4**. Alternatively, the reaction may involve an intramolecular metal ring-walking process.^{17,18,29,30,32–36} In order to distinguish between these distinctly different pathways, compound **2** or PhI (0.5 equiv) was added to a toluene-*d*₈ solution containing complex **3** and 2 equiv of PEt₃. Notably, compound **2** or PhI is present in a large excess, as compared with ligand **1** and Ni(PEt₃)_{*x*}, if these compounds will indeed be generated by a dissociation process. Subsequently, in situ ³¹P{¹H} NMR follow-up experiments at 278 K show the exclusive formation of complex **5**. No formation of complexes **4** and **6** or activation of PhI was observed (Scheme 2). PhI undergoes oxidative addition with Ni(PEt₃)₄ within ~10 min under similar reaction conditions, whereas the complete transformation of complex **3** → **5** takes ~4.5 h. Likewise, complex **4** forms almost exclusively complex **6** in the presence of compound **1**.

The reaction of Ni(PEt₃)₄ with compounds **1** and 4-R-PhI with R = H, OMe, or CF₃ (molar ratio 1:1:1) in toluene-*d*₈ at –65 °C for 2 h, followed by stirring at room temperature for an additional 2 h, resulted in metal insertion into the aryl–Br bond to generate complex **5** as the major compound (96%, R = H; 97%, R = OMe; 86%, R = CF₃). Metal insertion into the aryl–I bonds was also observed by ³¹P{¹H} NMR: 4% for Ni[(C₆H₅)₂(PEt₃)₂], 3% for Ni[(4-MeOC₆H₄)₂(PEt₃)₂], and 14% for Ni[(4-CF₃C₆H₄)₂(PEt₃)₂]. The latter three complexes were identified by the addition of authentic samples to the product solutions. ³¹P{¹H} NMR spectroscopy at –2 °C showed the initial quantitative formation of complex **3**. Neither continuous stirring for an additional 48 h nor heating the product solution at 45 °C for

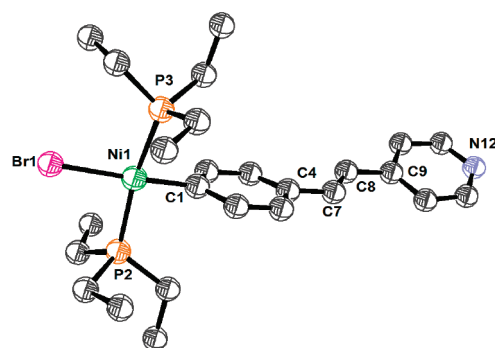
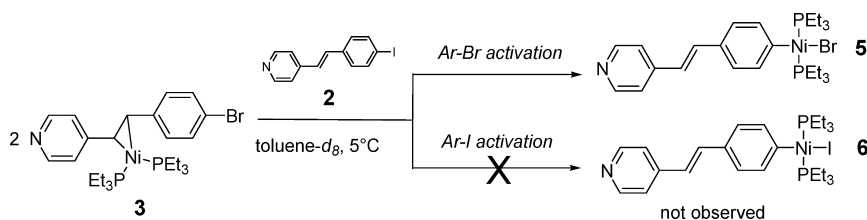
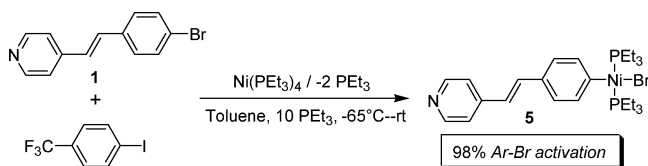


Figure 1. ORTEP diagram of complex **5** with thermal ellipsoids set at 50% probability. Hydrogen atoms are omitted for clarity. Selected bond lengths (Å) and angles (deg): Ni(1)–Br(1) 2.366(2), Ni(1)–P(2) 2.209(2), Ni(1)–P(3) 2.221(2), Ni(1)–C(1) 1.888(8), C(4)–C(7) 1.484(12), C(7)–C(8) 1.317(11), C(8)–C(9) 1.500(12), C(1)–Ni(1)–Br(1) 171.5(2), P(2)–Ni(1)–P(3) 168.02(11).

- (26) Yokoyama, A.; Yokozawa, T. *Macromolecules* **2007**, *40*, 4093.
 (27) Miyakoshi, R.; Shimon, K.; Yokoyama, A.; Yokozawa, T. *J. Am. Chem. Soc.* **2006**, *128*, 128.
 (28) Miyakoshi, R.; Yokoyama, A.; Yokozawa, T. *J. Am. Chem. Soc.* **2005**, *127*, 17542.
 (29) Keane, J. M.; Harman, W. D. *Organometallics* **2005**, *24*, 1786.
 (30) Harman, W. D. *Coord. Chem. Rev.* **2004**, *248*, 853.
 (31) For analogous Pd complexes, see: Burdeniuk, J.; Milstein, D. *J. Organomet. Chem.* **1993**, *451*, 213.

Scheme 2. Exclusive Formation of Complex **5** from **3** in the Presence of Compound **2** (0.5 equiv)^a

^a The addition of PhI instead of compound **2** to the reaction mixture also results in exclusive formation of complex **5**. Performing this reaction with complex **4** and compound **1** results in the formation of complex **6**. The experiments were performed in the presence of 2 equiv of PEt_3 .

Scheme 3. Directing Aryl–Halide Bond Activation via Ring-Walking^a

^a The formation of complex **5** was observed in the presence of 4- CF_3PhI . The quantitative formation of complex **3** was observed by $^{31}\text{P}\{^1\text{H}\}$ NMR spectroscopy prior to formation of complex **5**.

4 h changed the product distribution, demonstrating that complex **5** does not react with the aryl iodides to generate the observed minor products of aryl–I bond activation. It is remarkable that even nickel insertion into the aryl–Br bond occurs as a major pathway in the presence of the highly reactive 4- CF_3PhI . Apparently, the metal center is trapped, does not dissociate, and is directed toward the aryl–Br moiety because of the η^2 -coordination to the $-\text{C}=\text{C}-$ moiety of ligand **1**. The formation of **5** is clearly an intramolecular process. A reaction between two complexes **3** to afford free ligand **1** and a bimetallic complex, followed by the formation of **5** (from a bimetallic species), would be hampered by the presence of the aryl iodides. It is plausible that PhI, 4-MeOPhI, or 4- CF_3PhI reacts with complex **3** or a transient intermediate complex. One possible route may involve reversible PEt_3 dissociation from complex **3**, followed by reaction of the unsaturated metal complex with the aryl iodide. Indeed, performing the abovementioned reaction of **1** + 4- CF_3PhI with $\text{Ni}(\text{PEt}_3)_4$ in the presence of 10 equiv of PEt_3 increased the yield of complex **5** from 86% to 98%, as judged by $^{31}\text{P}\{^1\text{H}\}$ NMR spectroscopy (Scheme 3). A similar pathway seems to be operating for competing aryl–Br oxidative addition reactions with platinum and an azobenzene ligand.¹⁷ The intramolecular nature of the process **3** \rightarrow **5** is unambiguously demonstrated by the lack of metal transfer between ligands **1** and **2** and the abovementioned aryl–Br activation of ligand **1** as a major reaction pathway in the presence of aryl iodides (Schemes 2 and 3).

Further insight into the reaction pathway (**3** \rightarrow **5**, **4** \rightarrow **6**) and the rate-determining step is provided by the following competition experiments: the addition of a toluene- d_8 solution of compounds **1** and **2** (both 2 equiv) to a toluene- d_8 solution of $\text{Ni}(\text{PEt}_3)_4$ (1 equiv) at 278 K resulted in the initial formation of complexes **3** and **4** in an approximately 1.5:1 ratio, as judged by $^{31}\text{P}\{^1\text{H}\}$ NMR spectroscopy (Scheme 4A). The nature of the product ratio is not entirely clear; however, compound **1** is expected to coordinate slightly stronger to

the metal center for electronic reasons (e.g., compare Hammett constants for PhBr, $\sigma_p = 0.23$ vs PhI, $\sigma_p = 0.18$). In situ $^{31}\text{P}\{^1\text{H}\}$ NMR follow-up measurements in the presence of unreacted ligands **1** and **2** show the formation of complexes **5** and **6** with similar first-order rate constants: $k_{(\text{aryl-Br})} = 1.2 \times 10^{-4} \text{ s}^{-1}$ and $k_{(\text{aryl-I})} = 1.5 \times 10^{-4} \text{ s}^{-1}$, as shown in Scheme 4B. The final product distribution **5**:**6** = 1.5:1 is identical to the ratio of the kinetic complexes (**3**, **4**). Apparently, also under these reaction conditions, no ligand (**1**, **2**) scrambling occurs. The small difference between the rate constants ($k_{(\text{aryl-Br})}/k_{(\text{aryl-I})} \approx 0.8$) indicates that aryl–halide bond activation is not the rate-determining step. Furthermore, repeating this experiment with the addition of complex **3** (1 equiv) to the solution containing compounds **1** and **2** and complexes **3** and **4** (**3**:**4** = 1.5:1) afforded a product distribution of **5**:**6** = 2.5:1. It again appears that ligand (**1**, **2**) exchange and/or dissociation does not occur, which is fully in agreement with a ring-walking process. In addition, a reaction of free ligands (**1**, **2**) with complexes **3** and **4** to afford **5** and **6** directly can also be excluded.

The Eyring plots for both transformations (**3** \rightarrow **5** and **4** \rightarrow **6**) are identical within experimental errors (Figure 2). The very similar reaction profiles confirm that the aryl–halide activation process by nickel is not rate determining in the temperature range 265–285 K. This is in sharp contrast to our findings with platinum, in which a significant halide effect has been observed on the reaction kinetics.¹⁸ The low entropy values, ΔS^\ddagger , (i) exclude metal–ligand dissociation as the slow step and are consistent with either (ii) metal–ligand dissociation followed by aryl–halide oxidative addition as the rate determining step or (iii) an intramolecular process. The competition experiments rule out possibilities i and ii. Only an intramolecular process is fully in agreement with all our observations.

$^{31}\text{P}\{^1\text{H}\}$ NMR follow-up experiments were performed for the thermolysis of complex **3** in two different solvents and in the presence of excess PEt_3 (Figure 3). The solvent polarity (acetone vs toluene with dielectric constants of $\epsilon_r = 21$ vs 2.4, respectively)³⁷ or the presence of 2–10 equiv of PEt_3 does not affect the reaction kinetics. A “Meisenheimer-type” attack of the nickel center on the aryl–halide moiety or an

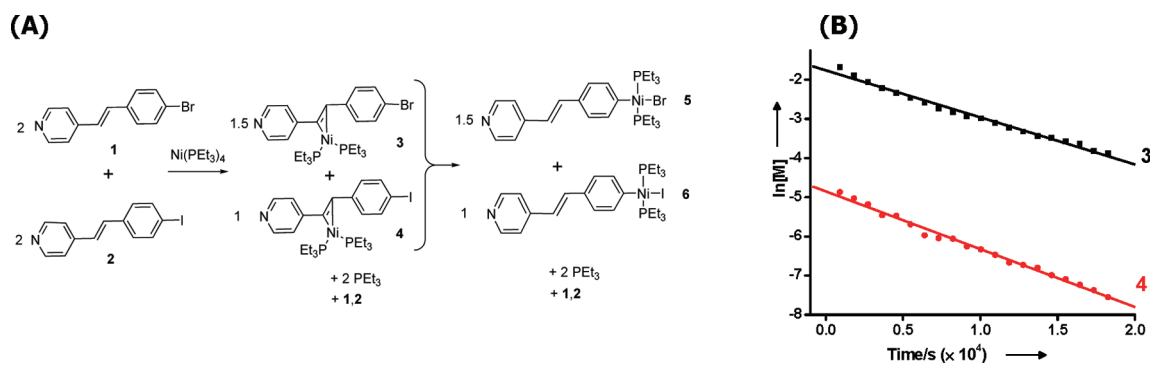
(32) Stanger, A.; Weismann, H. *J. Organomet. Chem.* **1996**, *515*, 183.

(33) Stanger, A.; Vollhardt, K. P. C. *Organometallics* **1992**, *11*, 317.

(34) Stanger, A. *Organometallics* **1991**, *10*, 2979.

(35) Siegel, J. S.; Baldrige, K. K.; Linden, A.; Dorta, R. *J. Am. Chem. Soc.* **2006**, *128*, 10644.

(36) Zingales, F.; Chiesa, A.; Basolo, F. *J. Am. Chem. Soc.* **1966**, *88*, 2707.

Scheme 4^a

^a (A) The competitive aryl-I and aryl-Br bond activation is controlled by η^2 -coordination of the metal center to compounds **1** and **2**. (B) In situ $^{31}\text{P}\{^1\text{H}\}$ NMR follow-up measurements of the conversions of **3** \rightarrow **5** (black line, $R^2 = 0.988$) and **4** \rightarrow **6** (red line, $R^2 = 0.990$) in toluene- d_8 at 278 K in the presence of free ligands (**1**, **2**) and PEt_3 .

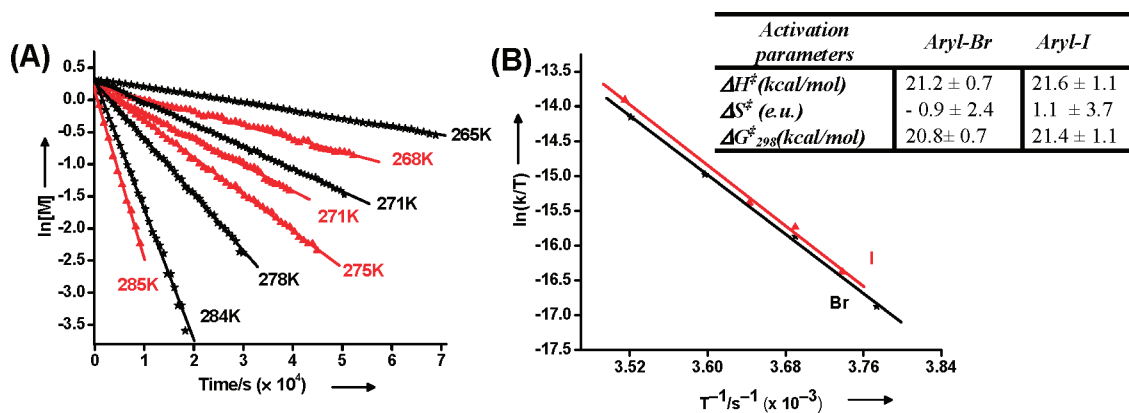


Figure 2. (A) In situ variable temperature $^{31}\text{P}\{^1\text{H}\}$ NMR follow-up measurements of the conversion of **3** \rightarrow **5** (black lines) and **4** \rightarrow **6** (red lines) in toluene- d_8 (15 mM). (B) Eyring plots of the conversion of **3** \rightarrow **5** (black line, $R^2 = 0.999$) and **4** \rightarrow **6** (red line, $R^2 = 0.996$).

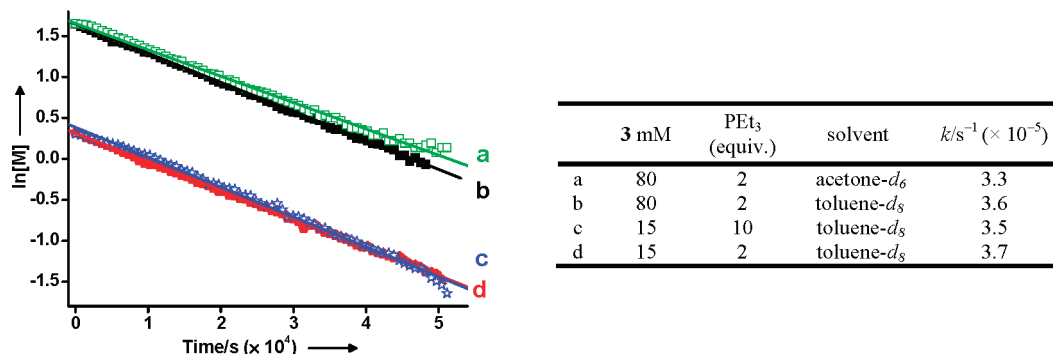


Figure 3. Representative in situ $^{31}\text{P}\{^1\text{H}\}$ NMR follow-up measurements of the thermolysis of complex **3** at 271 K.

electron-transfer process as the rate-limiting step would have been affected by the solvent.^{38–40} Tsou and Kochi established that the oxidative addition of $\text{Ni}(\text{PEt}_3)_4$ to aryl halides proceeds via an electron transfer process.⁴⁰ Such a mechanism is likely to be involved in various reactions such as the Ni-catalyzed Kharasch addition.⁴¹ Therefore, the thermolysis of complex **3** has also been followed by $^{31}\text{P}\{^1\text{H}\}$ NMR spectroscopy in the presence of 1 equiv of $n\text{-Bu}_4\text{NI}$.

If the reaction proceeds by intramolecular electron transfer in complex **3**,^{40–42} then ionic bromide should be formed as an intermediate, and the presence of iodide should lead to the formation of complex **6**. However, we only observed quantitative formation of complex **5**. In addition, we did not observe organic products derived from aryl radicals. The reaction **3** \rightarrow **5** is also not affected by the concentration within the range 15–80 mM, as expected for a first-order process. In addition, acetone is known to coordinate to unsaturated metal complexes,⁴³ which probably does not occur here or is not observable. Apparently, the transition

(37) *CRC Handbook of Chemistry and Physics*, 83rd ed.; Lide, D. R., Ed.; CRC Press: Boca Raton, FL, 2002–2003.

(38) Broxton, T. J.; Chung, R. P.-T. *J. Org. Chem.* **1990**, *55*, 3886.

(39) Mucsi, Z.; Szabó, A.; Hermecz, I.; Kucsman, A.; Csizmadia, I. G. *J. Am. Chem. Soc.* **2005**, *127*, 7615.

(40) Tsou, T. T.; Kochi, J. K. *J. Am. Chem. Soc.* **1979**, *101*, 6319.

(41) Gossage, R. A.; Gossage, R. A.; van der Kuil, L. A.; van Koten, G. *Acc. Chem. Res.* **1998**, *31*, 423.

(42) Hill, R. H.; Becalska, A.; Chiem, N. *Organometallics* **1991**, *10*, 2104.

(43) For example, see: Esteruelas, M. E.; Gómez, A. V.; Lahoz, F. J.; López, A. M.; Oñate, E.; Oro, L. A. *Organometallics* **1996**, *15*, 3423.

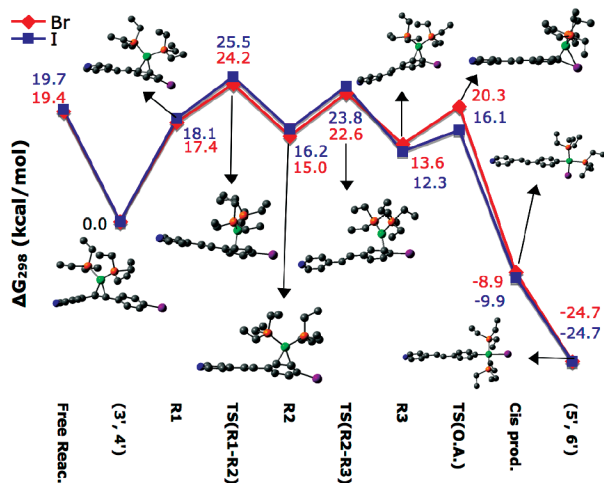


Figure 4. Reaction profile ($\Delta G_{298}^{\ddagger}$ kcal/mol, PCM(Benzene)-PBE0/SDB-cc-pVDZ//PBE0/SDD) for the ring-walking of Ni(PEt₃)₂ over the bromo- and iodo-stilbazole substrates (**1**, **2**). All H atoms have been omitted for clarity. (Atomic color scheme: C, gray; Ni, green; N, blue; Br or I, purple; P, orange.)

state of the slow step is nonpolar and most likely involves a system having two PEt₃ ligands bound to the metal center because solvent coordination and the presence of excess of PEt₃ appear not to play an experimentally observable role.

DFT calculations were performed to gain additional mechanistic insight into the experimental findings. The potential energy surfaces (PES) are simulated in benzene as the solvent for both systems (**1** → **5**, **2** → **6**) and are shown in Figure 4 along with a schematic illustration of the local minima and transition states that were located. As expected, the calculated structures located on the PES are qualitatively very similar to those reported for the related platinum system.¹⁸ Seven local minima were located on the PES. The local minimum (**3'**, **4'**), the reaction entry channel, corresponds to the experimentally observed η^2 -coordination of Ni(PEt₃)₂ to the $-\text{CH}=\text{CH}-$ moiety of ligands **1** and **2**. Three local minima involve η^2 -coordination of the Ni(PEt₃)₂ moiety to the C=C bonds of the phenyl ring (**R1**–**R3**). The two remaining local minima are the *cis* (**Cis prod**) and *trans* oxidative addition products (**5'**, **6'**). The transition states for ring-walking of Ni(PEt₃)₂ (**TS(R1–R2)**, **TS(R2–R3)**) and for the oxidative addition step (**TS(O.A.)**) were also located. Ligands **1** and **2** have very similar reaction profiles, with the exception of the expected higher barrier for aryl–Br activation: $\Delta(\text{TS(O.A.)}) \approx 4.2$ kcal/mol. Conversion of **R1** to **R2** via the transition state, **TS(R1–R2)**, occurs with relatively similar high energies for both the bromine (**3'**) and the iodine (**4'**) systems: $\Delta G_{298\text{K}}^{\ddagger} = 24.2$ and 25.5 kcal/mol, respectively. For both systems (**3'**, **4'**), this seems to be the RDS for the overall reaction. Moreover, the RDS for the bromine (**3'**) system is lower by 1.3 kcal/mol than that for the iodine system (**4'**). The transition state, **TS(3', 4'–R1)**, has not been located; however, the computational results suggest that a ring-walking process is kinetically accessible and in good agreement with the experimental findings.

Summary and Conclusions

In conclusion, selective nickel η^2 -coordination to a $-\text{CH}=\text{CH}-$ moiety is kinetically preferable over the oxidative addition of aryl–I and aryl–Br bonds. The overall process (**3** → **5** and **4** → **6**) proceeds via an intramolecular ring-walking mechanism. The aryl–halide bond activation by the nickel center is most probably not rate determining. It has been demonstrated that the coordination of the nickel center to the stilbazole model system can be used to direct the selectivity of aryl–halide bond activation processes. Selective activation of a strong aryl–Br bond occurs in the presence of relatively weak aryl–I bonds, as a result of metal–ligand interactions prior to the actual bond activation process. It is remarkable that selective aryl–Br activation by the d^{10} metal center occurs in the presence of a much weaker aryl–I bond (e.g., compare bond dissociation energies (BDEs) for Ph–Br = 80.5 kcal/mol vs Ph–I = 65.5 kcal/mol).³⁷ These findings and the mechanistic insight presented here, albeit with a model system, may have implications for future development of practical organic reactions involving selective functionalization of aryl–halides and other functional aryls by platinum group metals.

Experimental Details

General Procedures. All reactions were carried out under an N₂-filled M. Braun glovebox with H₂O and O₂ levels <2 ppm. Solvents were reagent grade or better, dried, distilled, and degassed before introduction into the glovebox, where they were stored over activated 4 Å molecular sieves. Deuterated solvents were purchased from Aldrich and were degassed and stored over 4 Å activated molecular sieves in the glovebox. Reaction flasks were washed with deionized (DI) water, followed by acetone, and then oven-dried prior to use. Mass spectrometry was carried out using a Micromass Platform LCZ 4000 mass spectrometer. Elemental analyses were performed by H. Kolbe, Mikroanalytisches Laboratorium, Mülheim an der Ruhr, Germany. Ligands **1**, **2**, and Ni(PEt₃)₄ were prepared by published procedures.⁴⁴

Spectroscopic Analysis. The ¹H, ¹³C, and ³¹P NMR spectra were recorded at 500.132, 125.77, and 202.46 MHz, respectively, on a Bruker Avance 500 NMR spectrometer. All chemical shifts (δ) are reported in parts per million and coupling constants (J) in hertz. The ¹H and ¹³C NMR chemical shifts are relative to tetramethylsilane; the resonance of the residual protons of the solvent was used as the internal standard h_1 (7.15 ppm, benzene; 7.09 ppm, toluene; 3.58 and 1.73 ppm, tetrahydrofuran) and all-*d* solvent peaks (128.0 ppm, benzene; 20.4 ppm, toluene; tetrahydrofuran, 67.6 and 25.3 ppm), respectively. ³¹P{¹H} NMR chemical shifts are relative to 85% H₃PO₄ in D₂O at $\delta = 0.0$ (external reference), with shifts downfield of the reference considered positive. All measurements were carried out at 298 K unless otherwise stated. Screw-cap 5 mm NMR tubes were used in NMR follow-up experiments. Et₃PO was used as the internal standard. Assignments in the ¹H and ¹³C{¹H} NMR were made using ¹H{³¹P} and ¹³C-DEPT-135 NMR.

³¹P{¹H} NMR Follow-up Measurements of the Formation of Complex **3.** Ni(PEt₃)₄ (30 mg, 0.056 mmol) was dissolved in 0.3 mL of toluene-*d*₈ and loaded in a 5 mm screw-cap NMR tube. Subsequently, a solution of 4-[2-bromo-phenyl]-vinyl]-pyridine (**1**)

(44) (a) Rodriguez, J. G.; Martin-Villamil, R.; Lafuente, A. *Tetrahedron* **2003**, *59*, 1021. (b) Schunn, R. A. *Inorg. Chem.* **1976**, *15*, 208.

(15 mg, 0.057 mmol) in 0.4 mL of toluene-*d*₈ was added at –75 °C. The tube was sealed, shaken, and immediately transferred into the precooled NMR machine at –75 °C. Follow-up ³¹P{¹H} NMR spectroscopy showed the selective formation of complex **3** and the concurrent disappearance of the starting materials. The reaction was completed after 4.5 h, yielding spectroscopically pure complex **3**. The formation of free PEt₃ (2 equiv) was observed during the reaction. No intermediates were observed. Complex **3** is stable in the temperature range –73 to –8 °C. For instance, it is stable in solution for at least 2 days at –40 °C and ~1 h at –8 °C. Performing the same reaction at –2 °C also resulted in the quantitative formation of complex **3** (after ~80 min). However, prolonged reaction times also showed the formation of complex **5**. For **3**: ¹H NMR (acetone-*d*₆ –60 °C, TMS): δ 0.84 (m, 18H, PCH₂CH₃), 1.51 (m, 12H, PCH₂CH₃), 3.60 (t, 2H, CH=CH, ³J_{HH} = 5.5 Hz), 7.63 (m, 4H, ArH, ³J_{HH} = 8.3 Hz), 7.64 (d, 2H, ArH, ³J_{HH} = 4.9 Hz), 8.59 (d, 2H, PyrH, ³J_{HH} = 4.9 Hz). ¹³C{¹H} NMR (acetone-*d*₆): δ 7.77 (m, PCH₂CH₃) 16.15 (m, PCH₂CH₃), 49.56 (d, η²-(CH=CH), ²J_{PC} = 17.7 Hz), 50.68 (d, η²-(CH=CH), ²J_{PC} = 16.9 Hz), 121.72, 122.39 (s, C_q, C–Br), 129.02, 131.56, 135.69 (C_q, s), 144.16 (C_q, s), 150.31. ³¹P{¹H} NMR (toluene-*d*₈): q, AB system δ_A = 16.9 (1P, ²J_{PP} = 39.7 Hz), δ_B = 18.3 (1P, ²J_{PP} = 39.7 Hz).

Formation of Complex 5. A solution of Ni(PEt₃)₄ (30 mg, 0.056 mmol) in THF (1 mL) was added to a solution of 4-[2-bromo-phenyl]-vinyl-pyridine (**1**) (15 mg, 0.057 mmol) in THF (0.5 mL) at room temperature. After 2 days, the volatiles were removed under vacuum followed by washing of the residue with dry, cold pentane (1 mL, –40 °C). The resulting solid was dissolved in a minimum quantity (~0.5 mL) of dry THF followed by a dropwise addition of dry pentane (~3 mL). Orange crystals, suitable for X-ray diffraction, were obtained upon slow evaporation of the solvent at room temperature (~80% yield). For **5**: ¹H NMR (C₆D₆): δ 1.01 (m, 18H, PCH₂CH₃), 1.39 (m, 12H, PCH₂CH₃), 6.76 (d, 1H, CH=CH, ³J_{HH} = 16.3 Hz), 6.88 (br, 2H, ArH), 7.05 (d, 1H, CH=CH, ³J_{HH} = 16.7 Hz), 7.45 (d, 2H, ArH, ³J_{HH} = 7.6 Hz), 7.07 (d, ArH, 2H, ³J_{HH} = 7.7 Hz), 8.56 (d, 2H, ³J_{HH} = 5.8 Hz, PyrH). ¹³C{¹H} NMR (C₆D₆): δ 8.06 (s, PCH₂CH₃), 14.67 (t, PCH₂CH₃, ¹J_{PC} = 14.3 Hz), 120.33, 122.98, 124.92, 129.61 (s, C_q), 133.78, 137.29, 144.62 (s, C_q), 150.52 (s), 162.39 (t, C_q, ¹J_{PC} = 66.6 Hz). ³¹P{¹H} NMR (C₆D₆): δ 11.24 (s, 2P). Calcd *m/e*: 555.14, found (M⁺ – Br) = 475.22. Anal. Calcd for C₂₅H₄₀BrNiP₂: C, 54.09; H, 7.26; N, 2.52. Found: C, 54.31; H, 7.11; N, 2.52.

³¹P{¹H} NMR Follow-up of the Formation of Complex 5 from Complex 3. A solution of Ni(PEt₃)₄ (30 mg, 0.056 mmol) in dry toluene-*d*₈ (0.4 mL) was added to a solution of 4-[2-bromo-phenyl]-vinyl-pyridine (**1**) (15 mg, 0.057 mmol) in dry toluene-*d*₈ (0.3 mL). The tube was shaken and immediately transferred into the precooled (–75 °C) NMR machine. Formation of complex **3** was observed by ³¹P{¹H} NMR spectroscopy after ~10 min (46% selective conversion of starting material). Nearly quantitative formation of complex **3** (98%) was observed after 4.5 h. The transformation **3** → **5** was monitored by VT ³¹P{¹H} NMR spectroscopy. The temperature was raised stepwise from –68 °C by 10 °C with time intervals of 30 min. At –8 °C, the formation of complex **5** was observed (~5% after 10 min). Follow-up ³¹P{¹H} NMR measurements were performed at –2 °C and showed the formation of complex **5** and the concurrent disappearance of complex **3**. No intermediates were observed during the reaction. After ~13.4 h, 83% of the starting material was selectively converted into compound **5**. Raising the temperature to 25 °C for ~2 h resulted in the quantitative formation of complex **5**. First-order linear fitting yielded $k_{271K} = 3.55 \times 10^{-5} \pm 1.1 \times 10^{-7} \text{ s}^{-1}$,

$R^2 = 0.994$). Reactions were also monitored in acetone-*d*₆ (0.080 mM, $k_{ac271K} = 3.23 \times 10^{-5} \pm 2.8 \times 10^{-7} \text{ s}^{-1}$, $R^2 = 0.996$), at lower concentrations (15 mM, $k_{271K} = 3.65 \times 10^{-5} \pm 2.8 \times 10^{-7} \text{ s}^{-1}$, $R^2 = 0.996$) and with excess of PEt₃ (15 mM, 10 equiv of PEt₃, $k_{271K} = 3.47 \times 10^{-5} \pm 1.0 \times 10^{-7} \text{ s}^{-1}$, $R^2 = 0.999$). Performing the reaction at various temperatures affords the following first-order rate constants: 15 mM, $k_{265K} = 1.2 \times 10^{-5} \pm 5.2 \times 10^{-8} \text{ s}^{-1}$, $R^2 = 0.999$; 15 mM, $k_{278K} = 8.71 \times 10^{-5} \pm 4.2 \times 10^{-7} \text{ s}^{-1}$, $R^2 = 0.999$; 15 mM, $k_{284K} = 2.02 \times 10^{-4} \pm 2.4 \times 10^{-6} \text{ s}^{-1}$, $R^2 = 0.997$.

³¹P{¹H} NMR Follow-up of the Formation of Complex 5 from Complex 3 in the Presence of Tetrabutylammonium Iodide. A screw-cap NMR tube containing a solution of Ni(PEt₃)₄ (3.5 mg, 0.0066 mmol) and tetrabutylammonium iodide (2.4 mg, 0.0065 mmol) in 0.4 mL of dry toluene-*d*₈ was cooled to –60 °C. Subsequently, a solution of 4-[2-bromo-phenyl]-vinyl-pyridine (**1**) (1.7 mg, 0.0065 mmol) in 0.3 mL of toluene-*d*₈ was added. The tube was shaken and immediately transferred into the precooled (5 °C) NMR machine. Quantitative formation of complex **3** was observed by ³¹P{¹H} NMR spectroscopy after ~5 min. Complex **3** undergoes selective aryl-halide oxidative addition to afford complex **5**. The reaction progress was monitored by ³¹P{¹H} NMR spectroscopy showing the disappearance of complex **3** and the concurrent formation of complex **5**. No other products such as complex **6** were observed. Complex **5** was identified by the addition of authentic sample. The reaction was completed in about 4 h.

Formation of Complex 4. Ni(PEt₃)₄ (7.8 mg, 0.015 mmol) was dissolved in 0.3 mL of toluene-*d*₈ and loaded in a 5 mm screw-cap NMR tube, which was equipped with a septum and was tightly closed using insulating tape and cooled until –60 °C. A solution of 4-[2-iodo-phenyl]-vinyl-pyridine (4.5 mg, 0.015 mmol) in 0.4 mL of toluene-*d*₈ (~30 °C) was added dropwise via a syringe into the sealed screw-cap NMR tube. Next, the tube was shaken and immediately transferred into the precooled (–2 °C) NMR machine. After ~5 min, the formation of complex **4** became visible by ³¹P{¹H} NMR (28% conversion of starting material). After 1.4 h at –2 °C, 97% conversion was observed. Complex **4** was the only observable product. No intermediates were observed during the reaction. Complex **4** slowly converts selectively to complex **6**. For **4**: ¹H NMR (THF-*d*₈, –13 °C, TMS): δ 0.93 (m, 18H, PCH₂CH₃), 1.14 (m, 12H, PCH₂CH₃), 3.41 (m, 2H, CH=CH, ³J_{HH} = 5.5 Hz), 6.97 (br, 2H, ArH), 7.00 (d, 2H, ArH, ³J_{HH} = 8.0 Hz), 7.35 (d, 2H, ArH, ³J_{HH} = 8.2 Hz), 8.11 (br, 2H, PyrH). ¹³C{¹H} NMR (THF-*d*₈, –13 °C): δ = 8.19 (br, PCH₂CH₃), 17.18 (ddd, ¹J_{PC} = 7.9 Hz, ³J_{PC} = 2.0 Hz, PCH₂CH₃), 49.56 (d, η²-(CH=CH), ¹J_{PC} = 17.9 Hz), 51.59 (d, η¹-(CH=CH), ¹J_{PC} = 17.2 Hz), 85.23 (br, C_q, C–I), 119.17, 126.82, 137.13, 137.13 (C_q, s), 148.23 (C_q, d), 149.35, 155.2 (C_q, br). ³¹P{¹H} NMR (toluene-*d*₈): q, AB system, δ_A = 17.0 (1P, ²J_{PP} = 39.6 Hz), δ_B = 18.3 (1P, ²J_{PP} = 39.6 Hz).

³¹P{¹H} NMR Follow-up Experiment of the Formation of Complex 6 from Complex 4. A solution of complex **4** (15 mM) was monitored by ³¹P{¹H} NMR spectroscopy at –2 °C. Formation of complex **6** became visible after ~30 min. ³¹P{¹H} NMR follow up measurements show the quantitative formation of complex **6** and the concurrent disappearance of complex **4** ($k_{271K} = 3.97 \times 10^{-5} \pm 2.5 \times 10^{-7} \text{ s}^{-1}$, $R^2 = 0.997$). After ~12 h, 90% conversion of starting materials was observed. The reaction was followed at various temperatures: 15 mM, $k_{268K} = 2.07 \times 10^{-5} \pm 2.4 \times 10^{-7} \text{ s}^{-1}$, $R^2 = 0.995$; 15 mM, $k_{275K} = 5.70 \times 10^{-5} \pm 2.5 \times 10^{-7} \text{ s}^{-1}$, $R^2 = 0.999$; 15 mM, $k_{285K} = 2.6 \times 10^{-4} \pm 4.2 \times 10^{-6} \text{ s}^{-1}$, $R^2 = 0.999$). For **6**: ¹H NMR (C₆D₆): δ 0.80 (m, 18H, PCH₂CH₃) 1.52–1.43 (m, 12H, PCH₂CH₃), 6.76 (dd, CH=CH, 1H, ³J_{HH} = 16.3 Hz), 7.09 (d, 1H, CH=CH, ³J_{HH} = 16.1 Hz), 7.16 (br, ArH,

2H), 7.19 (d, 2H, ArH, $^3J_{\text{HH}} = 8.1$ Hz), 7.51 (d, 2H, ArH, $^3J_{\text{HH}} = 7.5$ Hz), 9.70–9.56 (br, 2H, PyrH). $^{13}\text{C}\{^1\text{H}\}$ NMR (C_6D_6): δ 8.11 (s, PCH_2CH_3), 16.04 (t, PCH_2CH_3 , $^1J_{\text{PC}} = 13.3$ Hz), 123.89, 124.98, 126.96, 128.82, 130.20 (s, C_q), 133.14, 137.24 (s), 149.38 (br, C_q), 165.14 (t, C_q , $^1J_{\text{PC}} = 66.8$ Hz). $^{31}\text{P}\{^1\text{H}\}$ NMR (C_6D_6): δ 11.81 (s, 2P). Calcd *m/e*: 602.14, found = 602.85. Anal. Calcd for $\text{C}_{25}\text{H}_{40}\text{INNiP}_2$: C, 49.87; H, 6.7. Found: C, 49.46; H, 6.81.

Competition Experiments of $\text{Ni}(\text{PEt}_3)_4$ with 4-[2-Bromo-phenyl]-vinyl-pyridine (1) and 4-[2-Iodo-phenyl]-vinyl-pyridine (2). A screw-cap NMR tube containing a solution of $\text{Ni}(\text{PEt}_3)_4$ (3.5 mg, 0.0066 mmol) in 0.3 mL of dry toluene- d_8 was cooled to -60 °C. A solution of 4-[2-bromo-phenyl]-vinyl-pyridine (1) (3.4 mg, 0.013 mmol) and 4-[2-iodo-phenyl]-vinyl-pyridine (2) (4.0 mg, 0.013 mmol) in 0.4 mL of toluene- d_8 (-30 °C) was injected into the NMR tube (twofold excess of each ligand). The tube was shaken and immediately transferred into the precooled (5 °C) NMR machine. Complexes 3 and 4 in a ratio of 1.5:1 were observed by $^{31}\text{P}\{^1\text{H}\}$ NMR spectroscopy after ~ 5 min. No $\text{Ni}(\text{PEt}_3)_x$ ($x = 3, 4$) was observable. Both complex 3 and complex 4 undergo selective aryl–halide oxidative addition. The reaction progress was monitored by $^{31}\text{P}\{^1\text{H}\}$ NMR spectroscopy showing the disappearance of complexes 3 and 4 and the concurrent formation of complexes 5 and 6 (ratio 1.5:1). No intermediates were observed. The reaction was nearly completed in ~ 4 h with $k_{278\text{K}} = 1.2 \times 10^{-4} \pm 3.1 \times 10^{-6} \text{ s}^{-1}$ for $3 \rightarrow 5$ ($R^2 = 0.988$) and $k_{278\text{K}} = 1.5 \times 10^{-4} \pm 3.1 \times 10^{-6} \text{ s}^{-1}$ for $4 \rightarrow 6$ ($R^2 = 0.990$). Complexes 3–6 were identified by addition of authentic samples to the reaction mixture. The reaction was repeated; however, after the formation of complexes 3 and 4 (ratio 1.5:1), 1 equiv of complex 3 was added to the reaction mixture, resulting in a ratio 3:4 = 2.5:1. Quantitative formation of complexes 5 and 6 (ratio 2.5:1) was observed after 12 h at 0 °C.

Formation of Complex 5 from Complex 3 in the Presence of 4-[2-Iodo-phenyl]-vinyl-pyridine (2). A screw-cap NMR tube containing a solution of $\text{Ni}(\text{PEt}_3)_4$ (3.5 mg, 0.0066 mmol) in 0.3 mL of dry toluene- d_8 was cooled to -60 °C. Subsequently, a solution of 4-[2-bromo-phenyl]-vinyl-pyridine (1) (1.7 mg, 0.0065 mmol) in 0.3 mL of toluene- d_8 was added. The reaction progress was monitored by $^{31}\text{P}\{^1\text{H}\}$ NMR spectroscopy at -2 °C. The $\text{Ni}(\text{PEt}_3)_4$ was consumed after ~ 15 min, and quantitative formation of compound 3 was observed. Subsequently, a solution of 4-[2-iodo-phenyl]-vinyl-pyridine (2) (0.93 mg, 0.0030) in 0.2 mL of toluene- d_8 was added to the reaction mixture at -60 °C. The tube was shaken and immediately transferred into the precooled (5 °C) NMR machine. The reaction progress was monitored by $^{31}\text{P}\{^1\text{H}\}$ NMR spectroscopy showing the exclusive formation of complex 5 (93% conversion after ~ 4 h) and the concurrent disappearance of complex 3. Formation of complexes 4 and 6 was not observed.

Formation of Complex 6 from Complex 4 in the Presence of 4-[2-Bromo-phenyl]-vinyl-pyridine (1). A screw-cap NMR tube containing a solution of $\text{Ni}(\text{PEt}_3)_4$ (3.5 mg, 0.0066 mmol) in 0.3 mL of toluene- d_8 was cooled to -60 °C. Subsequently, a solution of 4-[2-iodo-phenyl]-vinyl-pyridine (2) (1.86 mg, 0.0061) in 0.3 mL of toluene- d_8 was added. The reaction progress was monitored by $^{31}\text{P}\{^1\text{H}\}$ NMR spectroscopy at -2 °C. The $\text{Ni}(\text{PEt}_3)_4$ was consumed after ~ 20 min, and quantitative formation of compound 4 was observed. Subsequently, a solution of 4-[2-bromo-phenyl]-vinyl-pyridine (1) (0.85 mg, 0.0033 mmol) in 0.2 mL of toluene- d_8 was added to the reaction mixture. The tube was shaken and immediately transferred into the precooled (5 °C) NMR machine. The reaction progress was monitored by $^{31}\text{P}\{^1\text{H}\}$ NMR spectroscopy showing the formation of complex 6 (92% after ~ 4 h) and the concurrent disappearance of complex 4. Traces of complex 5 (<5%) were observed.

Competition Experiments of $\text{Ni}(\text{PEt}_3)_4$ with Iodobenzene and Ligand 1. $\text{Ni}(\text{PEt}_3)_4$ (3.5 mg, 0.0066 mmol) was dissolved in 0.3 mL of dry toluene- d_8 and loaded in a 5 mm screw-cap NMR tube, which was equipped with a septum and was tightly closed using insulating tape. After cooling to -65 °C, a solution of 4-[2-bromo-phenyl]-vinyl-pyridine (1) (1.7 mg, 0.0065 mmol) and iodobenzene (1.35 mg, 0.0066 mmol) in 0.4 mL of dry toluene was added. Next, the tube was shaken and immediately transferred into the precooled (-2 °C) NMR machine. After 5 min, $^{31}\text{P}\{^1\text{H}\}$ NMR measurements showed the formation of complex 3 and the concurrent disappearance of $\text{Ni}(\text{PEt}_3)_4$. Quantitative formation of complex 3 was observed after ~ 80 min. Prolonged reaction times resulted in the formation of complex 5 and the concurrent disappearance of compound 3. After 14 h, $^{31}\text{P}\{^1\text{H}\}$ NMR analysis showed full conversion of $\text{Ni}(\text{PEt}_3)_4$, free PEt_3 , and the formation of complexes 5 (96%) and $\text{NiI}(\text{C}_6\text{H}_5)(\text{PEt}_3)_2$ (4%). No intermediates were observed during the reaction. The product distribution is stable at room temperature for at least 48 h and for 4 h at 45 °C. Apparently, complexes 5 and $\text{NiI}(\text{C}_6\text{H}_5)(\text{PEt}_3)_2$ are thermodynamically stable and do not interconvert.

Competition Experiments of $\text{Ni}(\text{PEt}_3)_4$ with 1-Iodo-4-methoxy-benzene and Ligand 1. A cold solution (-65 °C) of $\text{Ni}(\text{PEt}_3)_4$ (3.5 mg, 0.0066 mmol) in 0.3 mL of toluene- d_8 was mixed with a cold solution of 1-iodo-4-methoxy-benzene (1.54 mg, 0.0066 mmol) and 4-[2-bromo-phenyl]-vinyl-pyridine (1) (1.7 mg, 0.0065 mmol) in 0.4 mL of toluene- d_8 . The reaction mixture was kept at -65 °C for 2 h and then allowed to attain room temperature (~ 2 h). $^{31}\text{P}\{^1\text{H}\}$ NMR measurements showed the formation of complexes 5 (97%) and $\text{NiI}(4\text{-MeO-C}_6\text{H}_4)(\text{PEt}_3)_2$ (3%). No other products were observed.

Competition Experiments of $\text{Ni}(\text{PEt}_3)_4$ with 1-Iodo-4-trifluoromethyl-benzene and Ligand 1. A cold solution (-65 °C) of $\text{Ni}(\text{PEt}_3)_4$ (3.5 mg, 0.0066 mmol) in 0.3 mL of dry toluene- d_8 was mixed with a cold solution of 1-iodo-4-trifluoromethyl-benzene (1.79 mg, 0.0066 mmol) and 4-[2-bromo-phenyl]-vinyl-pyridine (1) (1.87 mg, 0.0072 mmol) in 0.4 mL of toluene- d_8 . The reaction mixture was kept at -65 °C for 2 h and then allowed to attain room temperature (~ 2 h). $^{31}\text{P}\{^1\text{H}\}$ NMR analysis showed full conversion of $\text{Ni}(\text{PEt}_3)_4$, free PEt_3 , and the formation of complexes 5 (86%) and $\text{NiI}(4\text{-CF}_3\text{-C}_6\text{H}_4)(\text{PEt}_3)_2$ (14%). No other products were observed. Repeating this experiment with the addition of 10 equiv of PEt_3 (7.7 mg, 0.066 mmol) to the reaction mixture suppressed the formation of $\text{NiI}(4\text{-CF}_3\text{-C}_6\text{H}_4)(\text{PEt}_3)_2$ to 2%.

X-ray Analysis of Complex 5. Crystal data: $\text{C}_{25}\text{H}_{40}\text{NP}_2\text{BrNi}$, $M = 555.14$, orthorhombic, space group $Pna2_1$, $a = 16.112(3)$, $b = 14.717(3)$, $c = 11.515(2)$ Å, $Z = 4$, $\rho_{\text{calcd}} = 1.350 \text{ g cm}^{-3}$, 16 170 reflections measured, 2747 unique ($R_{\text{int}} = 0.098$, $2\theta_{\text{max}} = 50.7^\circ$), final $R = 0.046$ ($R_w = 0.091$) for 2622 reflections with $I > 2\sigma(I)$ and $R = 0.061$ ($R_w = 0.098$) for all data.

Computational Details

All calculations were carried out using Gaussian 03, Revision C.01.⁴⁵ The PBE0 DFT exchange–correlation functional was used for the investigation. This functional, also known as PBE1PBE, is the hybrid variant (25% HF exchange) of PBE (Perdew, Burke, and Ernzerhof's)⁴⁶ nonempirical GGA functional. With this functional, two basis set-RECP (relativistic effective core potential) combinations were used. The first, denoted SDD, is a combination of the Huzinaga–Dunning double- ζ basis set on lighter elements with the Stuttgart–Dresden basis set-RECP combination on transition metals.⁴⁷ The second donated SDB-cc-pVDZ

corresponds to the Dunning cc-pVDZ basis set⁴⁸ on the main group elements and the Stuttgart–Dresden basis set-RECP on the transition metals with additional 2f1g-type polarization exponents given in ref 49. Geometries were optimized using the former basis set with the default pruned (75 302) grid, whereas the binding energies were calculated with the latter basis set and the “ultrafine” grid (i.e., a pruned (99 590) grid). This level of theory is conventionally denoted as PBE0/SDB-cc-pVDZ//PBE0/SDD. Bulk solvent effects⁵⁰ were approximated by single point PBE0/SDB-cc-pVDZ energy calculations using a polarized continuum (overlapping spheres)

model (PCM)^{51–53} with benzene as the solvent. The connectivity of the transition states was confirmed by performing intrinsic reaction coordinate (IRC) calculations.^{54–56} Equilibrium geometries were verified to have all real harmonic frequencies and transition states to have one imaginary frequency.

Acknowledgment. This research was supported by the Helen and Martin Kimmel Center for Molecular Design, the Lise Meitner-Minerva Center for Computational Quantum Chemistry, the Israel Science Foundation (ISF), the German Federal Ministry for Education and Research (BMBF), and the Minerva Junior Research Groups (MJRG) program. M.E.vd.B. is the incumbent of the Dewey David Stone and Harry Levine Career Development Chair, while J.M.L.M. is the Baroness Thatcher Professor of Chemistry. We thank Mr. D. Strawser for performing preliminary experiments.

Supporting Information Available: Crystallographic data (CIF) for complex **5**. This material is available free of charge via the Internet at <http://pubs.acs.org>.

IC702289N

- (45) Frisch, M. J. T.; G. W.; Schlegel, H. B.; Scuseria, G. E. R.; M. E.; Cheeseman, J. R.; Montgomery J. A., Jr.; Vreven, T.; Kudin, K. N.; Burant, J. C.; Millam, J. M.; Iyengar, S. S.; Tomasi, J.; Barone, V.; Mennucci, B.; Cossi, M.; Scalmani, G.; Rega, N.; Petersson, G. A.; Nakatsuji, H.; Hada, M.; Ehara, M.; Toyota, K.; Fukuda, R.; Hasegawa, J.; Ishida, M.; Nakajima, T.; Honda, Y.; Kitao, O.; Nakai, H.; Klene, M.; Li, Z.; Knox, J. E.; Hratchian, H. P.; Cross, J. B.; Adamo, C.; Jaramillo, J.; Gomperts, R.; Stratmann, R. E.; Yazyev, O.; Austin, A. J.; Cammi, R.; Pomelli, C.; Ochterski, J. W.; Ayala, P. Y.; Morokuma, K.; Voth, G. A.; Salvador, P.; Dannenberg, J. J.; Zakrzewski, V. G.; Dapprich, S.; Daniels, A. D.; Strain, M. C.; Farkas, O.; Malick, D. K.; Rabuck, A. D.; Raghavachari, K.; Foresman, J. B.; Ortiz, J. V.; Cui, Q.; Baboul, A. G.; Clifford, S.; Cioslowski, J.; Stefanov, B. B.; Liu, G.; Liashenko, A.; Piskorz, P.; Komaromi, I.; Martin, R. L.; Fox, D. J.; Keith, T.; Al-Laham, M. A.; Peng, C. Y.; Nanayakkara, A.; Challacombe, M.; Gill, P. M. W.; Johnson, B.; Chen, W.; Wong, M. W.; Gonzalez, C.; Pople, J. A. *Gaussian 03*, Revision C.01; Gaussian, Inc.: Wallingford, CT, 2004.
- (46) Perdew, J. P.; Burke, K.; Ernzerhof, M. *Phys. Rev. Lett.* **1996**, *77*, 3865.
- (47) Dolg, M. Effective Core Potentials. In *Modern Methods and Algorithms of Quantum Chemistry*; Grotendorst, J., Ed.; John von Neumann Institute for Computing: Julich, Germany, 2000; Vol. 1, p 479.
- (48) Dunning, T. H., Jr. *J. Chem. Phys.* **1989**, *90*, 1007.
- (49) Martin, J. M. L.; Sundermann, A. *J. Chem. Phys.* **2001**, *114*, 3408.
- (50) Cramer, C. J. *Essentials of Computational Chemistry: Theories and Models*; John Wiley & Sons: Chichester, U.K., 2002; p 347.
- (51) Miertuš, S.; Scrocco, E.; Tomasi, J. *Chem. Phys.* **1981**, *55*, 117.
- (52) Miertuš, S.; Tomasi, J. *Chem. Phys.* **1982**, *65*, 239.
- (53) Cossi, M.; Barone, V.; Cammi, R.; Tomasi, J. *Chem. Phys. Lett.* **1996**, *255*, 327.
- (54) Fukui, K. *Acc. Chem. Res.* **1981**, *14*, 363.
- (55) Gonzalez, C.; Schlegel, H. B. *J. Chem. Phys.* **1989**, *90*.
- (56) Gonzalez, C.; Schlegel, H. B. *J. Phys. Chem.* **1990**, *94*, 5523.